Non-Surgical Carpal Arch Space Augmentation for Median Nerve Decompression

Zong-Ming Li[1]

Departments of Orthopaedic Surgery and
Biomedical Engineering,
Hand Research Laboratory,
University of Arizona,
Tucson, AZ 85724
e-mail: lizongming@arizona.edu

The carpal tunnel is a tightly bounded space, making the median nerve prone to compression and eventually leading to carpal tunnel syndrome. Carpal tunnel release surgery transects the transverse carpal ligament to expand the tunnel arch space, decompress the median nerve, and relieve the associated symptoms. However, the surgical procedure unavoidably disrupts essential anatomical, biomechanical and physiological functions of the wrist, potentially causing reduced grip strength, pillar pain, carpal bone instability, scar tissue formation, and perineural fibrosis. It is desirable to decompress the median nerve without surgically transecting the transverse carpal ligament. This paper is to review several approaches we have developed for nonsurgical carpal arch space augmentation (CASA), namely, radio ulnar wrist compression, muscle-ligament interaction, palmar pulling, and collagenolysis of the transverse carpal ligament. Briefly summarized is the research work on the CASA topic about theoretical considerations, in vitro and in situ experiment, computational modeling, and human subject studies with asymptomatic and carpal tunnel syndrome hands. [DOI: 10.1115/1.4056651]

Keywords: carpal tunnel syndrome, carpal arch space augmentation, Non-surgical intervention

1 The Carpal Tunnel and Carpal Tunnel Syndrome

The carpal tunnel at the wrist is formed by the carpal bones and intercarpal ligaments at the medial, lateral, and dorsal aspects. The volar boundary of the tunnel is bounded by the transverse carpal ligament, a dense fibrous tissue [1]. The tunnel is packed with the median nerve, nine tendons of the extrinsic flexors of the thumb and fingers, and other connective tissues. The thenar muscles, although outside the tunnel, interact with the transverse carpal ligament and have implications on the carpal arch.

The crowded contents within the confined carpal tunnel space make the median nerve vulnerable to compression, eventually leading to carpal tunnel syndrome. Carpal tunnel syndrome is the most common compression neuropathy and the most commonly diagnosed hand disorder affecting between 3 and 5% of the population in the United States and around the world [2,3]. Symptoms of this syndrome include tingling, numbness, pain, loss of grip and pinch strength, and lack of digit coordination in the hand. Despite the widespread burden of carpal tunnel syndrome, clinical management of carpal tunnel syndrome can be challenging for both physicians and patients. Current treatment options can be categorized as either conservative or surgical interventions. Non-invasive methods to alleviate the symptoms include nonsteroidal anti-inflammatory drugs, corticosteroids, stretching, splinting, massage, and laser treatment [4]. Carpal tunnel release surgery has existed for nearly a century without fundamental changes and is still considered the standard solution to treat carpal tunnel syndrome. The surgery involves transection of the transverse carpal ligament to remove the constraint of the tunnel, expand the tunnel space, decompress the stressed median nerve, and therefore relieve the associated symptoms [5]. However, the surgical procedure unavoidably disrupts essential anatomical, biomechanical and physiological functions of the wrist [6,7] and can cause reduced grip strength, pillar pain, carpal bone instability, scar tissue formation, and perineural fibrosis [8]. These side effects, as pointed out by Kiritsis and Kline, "continue to challenge hand surgeons to find a way to decompress the median nerve adequately at the wrist and avoid the mechanical consequences of dividing the (transverse carpal ligament)" [9].

We asked the question: can we decompress the median nerve of patients with carpal tunnel syndrome without surgically transecting the transverse carpal ligament? Guided by this question, we developed several approaches for carpal arch space augmentation (CASA), namely, radio ulnar wrist compression, muscle-ligament interaction, palmar pulling, and collagenolysis of the transverse carpal ligament. This paper is a review of our research work on the CASA topic about theoretical considerations, in vitro and in situ experiment, computational modeling, and human subject studies with asymptomatic and carpal tunnel syndrome hands.

2 Radio Ulnar Wrist Compression for Carpal Arch Space Augmentation

Initially motivated by the belief of expanding the carpal tunnel through stretching the transverse carpal ligament, we investigated the effects of applying palmarly directed forces to the ligament from inside the carpal tunnel [10]. We performed an experiment using cadaveric hand specimens dissected to evacuate the carpal tunnel and to expose the ligament. A custom lever device was built to apply forces up to 200 N to the ligament. The force application caused the ligament to form arches with an increase, on average, in cross-sectional areas of $33.3\,mm^2$ at 10 N and $48.7\,mm^2$ at 200 N, representing respective increases of 22.4% and 32.8% relative to the initial carpal tunnel area. However, the ligament length remained unchanged under the applied forces. We were puzzled; it turned out that the arch formation was due to the narrowing of the arch width, which resulted from the migration of the bony insertion sites of the ligament. This finding has led us to decades of research about carpal arch narrowing for CASA.

A Triangle Model Explanation of Carpal Arch Formation. We used a geometrical model of the carpal tunnel to explain the relationships among the arch width, height, and area of the
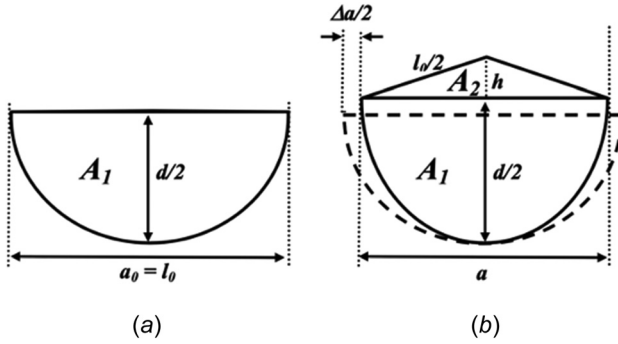
Fig. 1 Geometric representation of the cross section of the carpal tunnel: (a) Initial carpal tunnel without arch and (b) arch formation by arch width narrowing assuming a constant arch length

experimental data [10]. The transverse carpal ligament was relatively flat without a force applied to it, which means that the arch width (a_0) is equal to the ligament length (l_0) (Fig. 1(a)). A carpal arch was formed when a force was applied to the ligament. The arch formation can be achieved by moving the ligament edges toward each other (i.e., narrowing the arch. Fig. 1(b)). The ligament arch was assumed to be an isosceles triangle, which was closely approximated given that the force application is concentrated on the middle point of the ligament.

Assuming a constant ligament length (l_0), the base of the isosceles triangle is $a = l_0 - \Delta a$, where Δa is amount of arch width narrowing. The height of the isosceles triangle (h) and the arch area (A_2) are $\sqrt{(\frac{l_0}{2})^2 - (\frac{l_0 - \Delta a}{2})^2}$ and $\frac{1}{2} \times (l_0 - \Delta a) \times \sqrt{(\frac{l_0}{2})^2 - (\frac{l_0 - \Delta a}{2})^2}$, respectively. In this case, the arch height and arch area are functions of arch width narrowing (Δa). The initial values of the ligament length and arch width are $l_0 = a_0 = 22.0$ mm. The modeling results show that the arch height and the arch area are sensitive to arch width narrowing (Fig. 2). A small arch width narrowing leads to a relatively large increase in arch height (h) and arch area (A_2) (Fig. 2). For example, a decrease of
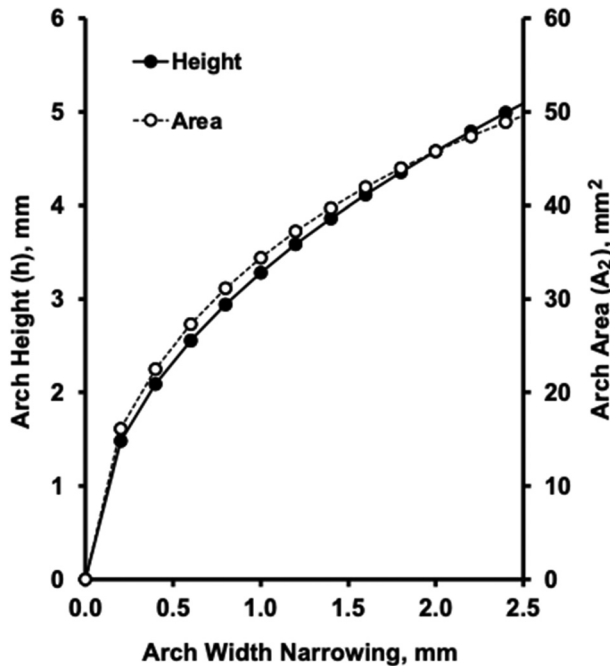

Fig. 2 Arch height (h) and area (A_2) changes due to arch width narrowing

0.2 mm in arch width produces an increase of 1.5 mm in arch height and 16.1 mm^2 in arch area. An increase of 4.6 mm in arch height and 45.8 mm^2 in arch area was formed with 2.0 mm arch width narrowing; that is a dramatic increase of carpal space considering the cross-sectional area of carpal tunnel and median nerve is about 160 mm^2 and 10 mm^2, respectively.

How does the carpal width narrowing affect the cross-sectional area composed by the carpal bones (A_1)? For a geometrical model, the bony cross section of the carpal tunnel (A_1) is assumed to be a semi-ellipse (Fig. 1), whose principal axes are represented by the carpal arch width (a) and twice the carpal depth ($d/2$). The area (A_1) can be calculated as $\frac{1}{2} \times \pi \times \frac{a}{2} \times \frac{d}{2}$, and the perimeter of the half-ellipse (excluding the arch width, a) as $\frac{1}{2} \times \pi \times [3 \times (\frac{a}{2} + \frac{d}{2}) - \sqrt{(\frac{3a}{2} + \frac{d}{2})(\frac{a}{2} + \frac{3d}{2})}]$. With the assumption that the perimeter of the ellipse is constant, d covaries with a. As such, A_1 is a function of the change in a. However, A_1 is insensitive to the change of a. Using the average carpal tunnel depth of 9.5 mm for comparison, the area (A_1) fluctuates only slightly (within 1.3 mm^2) when the tunnel width (a) is decreased by 0-2.5 mm. Therefore, the increase in total area is mainly attributable to the formation of the carpal arch.

A Parabolic Model of Carpal Arch. In physiological state, the carpal arch height can be assumed to follow a parabolic function: $y = a + bx^2$ (Fig. 3). For a given initial arch width (W) and arch height (H), the carpal arch can be expressed as the following function:

$$y = H - 4H \left(\frac{x}{W} \right)^2 \tag{1}$$

With the parabola function, arch area (A) and carpal arch length (L) can be derived as a function of the initial arch width (W) and initial arch height (H) as in the following:

$$L = \int_{-\frac{W}{2}}^{+\frac{W}{2}} \sqrt{1 + \left(\frac{dy}{dx} \right)^2} \, dx$$
$$= \frac{1}{2} \sqrt{W + 16H^2} + \frac{W^2}{8H} ln \left[\frac{4H + \sqrt{W + 16H^2}}{W} \right] \tag{2}$$

$$A = \int_{-\frac{W}{2}}^{+\frac{W}{2}} y \, dx = \frac{2}{3} HW \tag{3}$$

A constraint of the geometrical model is that the arch length, as determined by initial arch width (W) and initial arch height (H), remains invariant during carpal arch manipulation. This
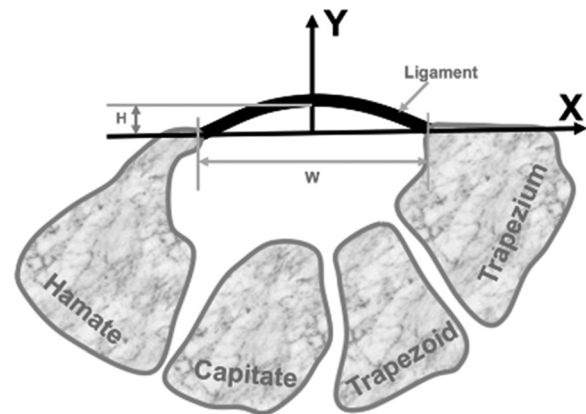

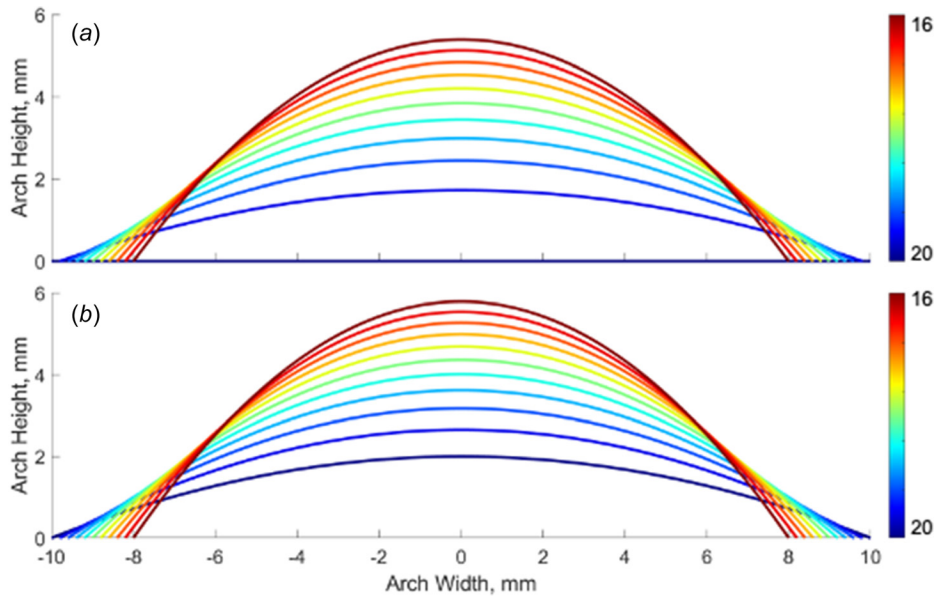**Fig. 3 Carpal arch height approximation by a parabola function**

Fig. 4   Arch formation as arch width decreases from 20 mm (blue) to 16 mm (red) with initial carpal height of 0 mm (*a*) and 2 mm (*b*)

assumption of constant arch length is valid based on our previous study showing that the ligament length remained constant under the palmarly directed forces [10]. In the simplest scenario, we assume an initial arch width of 20 mm and a flattened carpal arch, which indicates that the arc length equals to the arch width. We show that a decrease in arch width leads to large carpal arch formation (Fig. 4). For example, when the arch width changed from 20 to 16 mm, the height is 5.4 mm, and the area is 57.5 mm^2 (Fig. 4(*a*)) Arch height and area increase nonlinearly as a function of arch width narrowing. Moreover, the arch has a smaller increase for a given arch width narrowing as the initial arch height increases. For example, with an initial arch height of 2 mm, a gain of additional arch height and area were 3.8 mm and 35.1 mm^2, respectively, with 4 mm arch width narrowing from 20 to 16 mm (Fig. 4(*a*)).

A Constant Perimeter Model of Carpal Tunnel Cross Section. Imagine that the perimeter of two-dimensional cross section is made of a string with unchangeable length. We can reconfigure it to make different shapes with the same perimeter but with many different areas (e.g., circle, an ellipse, square, and equilateral triangle, Fig. 5). It is a theorem that a circle has the maximum area enclosed by any shape with the same perimeter length. Assume the perimeter of 50 mm of the cross section of distal carpal tunnel, and fitted ellipse of the tunnel has an aspect ratio of approximately 2 to 1 [11]. This elliptic cross section has an area of 167 mm^2. If we make the cross section less flattened or more circular, the area will increase and reach to maximal of 198 mm^2 when the shape is a circle. The carpal tunnel area has a potential to increase its area by 31 mm^2 or 16% from an ellipse with aspect ratio of 2 to a circle.

Cadaveric Experiments. The geometrical modeling demonstrates the theoretical plausibility of increasing carpal tunnel cross-sectional area. Our next research question was to what extent the carpal tunnel shape is deformable considering that the structure is formed by irregularly shaped carpal bones interconnected by numerous ligaments. We performed cadaveric experiments to understand the structural deformability of the wrist [12–16]. In one study, we determined the three-dimensional stiffness characteristics of the carpal arch using displacement perturbations [13]. An instrumented robot arm applied three-dimensional displacement perturbations to the ridge of trapezium,

and corresponding reaction forces were collected. The displacement-force data were used to determine a three-dimensional stiffness matrix using least squares fitting. Eigen decomposition of the stiffness matrix was used to identify the magnitudes the principal components of 16.46, 3.17, and 1.67 N/mm and their orientations in oblique directions. In another study, we investigated the angular rotations of the distal carpal joints as the arch width was adjusted [14]. The carpal arch width was narrowed by 2 and 4 mm while the bone positions were tracked by a marker-based motion capture system. We found that contributions of individual carpal bones were different with the hamate-capitate joint range of motion greater than that of capitate-trapezoid and trapezoid-trapezium joints. Yet in another study, we investigated the morphological changes of the carpal arch as a result of carpal arch width narrowing in cadaveric hands [15]. The carpal arch width was narrowed by a custom apparatus and cross-sectional ultrasound images were acquired. The carpal arch height and area were quantified as the carpal arch width was narrowed. Correlation and regression analyses were performed for the carpal arch height and area with respect to the carpal arch width. We found that the carpal arch was more convex as the
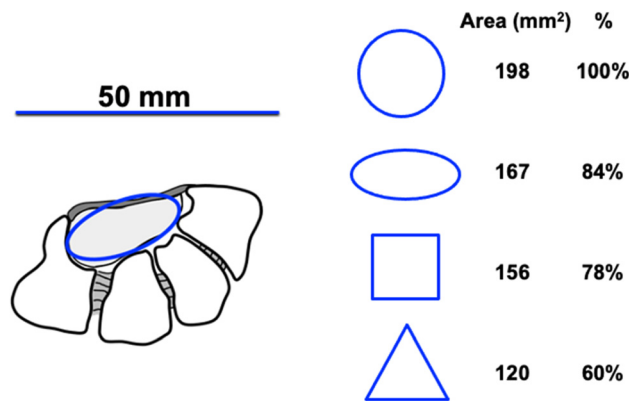

Fig. 5   A circle is the shape forming the greatest area for a given perimeter length. Note that for the elliptic shape is assumed to have an aspect ratio (i.e., major axis length divided by minor axis length) of 2 which approximates the carpal tunnel shape.

carpal arch width was narrowed. The carpal arch height and area negatively correlated with the carpal arch width, with correlation coefficients of an average of −0.974 and −0.925, respectively. We confirmed that the carpal arch width is manipulatable to an extent that leads to increased carpal arch height and area.

Experimental Studies With Human Hands. We continued with the experimental studies on human subjects with asymptomatic and carpal tunnel syndrome hands [17,18]. We investigated the morphological and positional changes of the carpal arch and median nerve while compressive forces were applied in the radio ulnar direction across the wrist. A pressure system was developed to apply transverse compression at the distal level of the carpal tunnel (Fig. 6(a)). Ultrasound images of the carpal tunnel and its contents were captured at the distal tunnel level prior to force application and during force applications of 10 and 20 N. With applied force, the carpal arch width decreased, while the carpal arch height, area, and curvature increased. The median nerve shape became more rounded as the compressive force magnitude increased, reflected by decreases in the nerve's flattening ratio and increases in its circularity. The applied force also resulted in nerve displacement in the radial-volar direction. This study demonstrates that noninvasively applying radio ulnar compressive force across the wrist may potentially provide relief of median nerve compression to patients suffering from carpal tunnel syndrome.
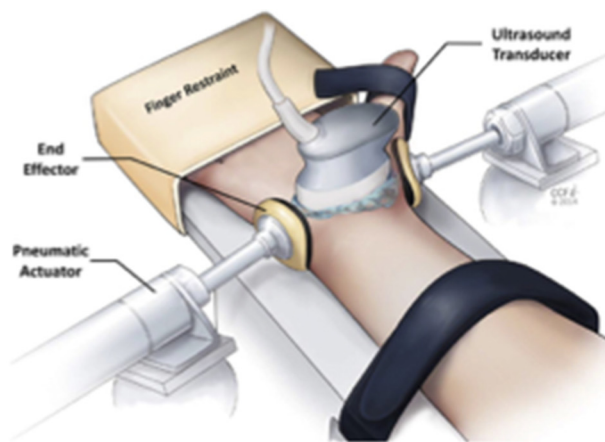
(a)
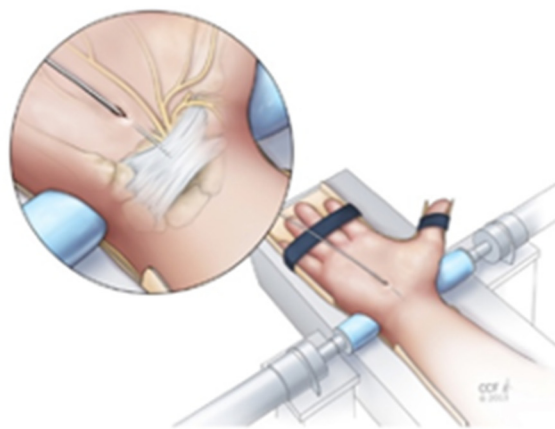
(b)

Fig. 6 In vivo ultrasound imaging (a) tunnel pressure measurement (b) during radio ulnar compression of the wrist

Carpal tunnel syndrome is known to be associated with elevated carpal tunnel pressure that causes compression of the median nerve in the tunnel. In a normal physiological state, the pressure within the carpal tunnel is relatively low at about 15 mmHg [19]; but in patients with carpal tunnel syndrome, the pressure can be >200 mmHg [20,21]. We were interested in the changes of carpal tunnel pressure in carpal tunnel syndrome patients in response to radio ulnar wrist compression [22]. This study was performed in the operating room prior to mini-open carpal tunnel release surgery. A pressure catheter (Millar, Inc., Houston, TX) was inserted into the carpal tunnel via the palmar incision (Fig. 6(b)). The compression system applied radio ulnar compressive forces of 10 N and 20 N across the distal level of the carpal tunnel. We found that the baseline carpal tunnel pressure ranged from 48.2 to 106.1 mmHg among the patients, with an average of 76.6 mmHg. As the compressive force increased, carpal tunnel pressure decreased. When the force was 10 N, the carpal tunnel pressure dropped to an average of 65.6 mmHg, a decrease of 11.0 mmHg or 14.7%. When 20 N of force was applied, the carpal tunnel pressure dropped to an average of 59.0 mmHg, a decrease of 17.6 mmHg or 24.2%. We also found that the extent of the pressure drop during force application was variable in the tested wrists, ranging from 3% to 55%. The variability of the pressure drop may be associated with patient factors (e.g., difference in carpal tunnel severity, baseline pressure, and wrist anatomy) and force application factors (e.g., location and direction of force). Of note, this study was recognized "Best of ORS" in the hand and wrist category in Orthopedic Research Society Annual Meeting and was highlighted at the American Academy of Orthopedic Surgeons (AAOS) Annual Meeting in 2016.

Also, we examined median nerve longitudinal mobility within the carpal tunnel of carpal tunnel syndrome patients while the radio ulnar compression was applied [23,24]. Dynamic ultrasound images of the carpal tunnel during finger motion captured longitudinal median nerve motion during radio ulnar wrist compression force application. We found that median nerve mobility was not affected by radio ulnar wrist compression in healthy subjects but improved by 10 N radio ulnar wrist compression in carpal tunnel syndrome patients. Analysis of segmental median nerve mobility in carpal tunnel syndrome patients showed improved mobility in the proximal tunnel section under the wrist compression force condition. It appears that moderate radio ulnar wrist compression force application helps restore impaired median nerve mobility, which is a sign of released constraint of the median nerve in the carpal tunnel.

Computational Modeling. We investigated the optimal force direction for maximal carpal tunnel cross-sectional area using a finite element model [25]. A planar geometric model of carpal bones at the hamate level was reconstructed with intercarpal joint spaces filled with a linear elastic surrogate tissue. Experimental data with discrete carpal tunnel pressures and corresponding carpal bone movements were used to obtain the material properties of the surrogate tissue by inverse finite element analysis. The resulting model was used to simulate changes of carpal arch widths and areas with directional variations of a unit force applied at the hook of hamate. Simulation of force applications showed that carpal arch width and area were dependent on the direction of force application, and maximal area occurred at volar-radial direction with respect to the hamate-to-trapezium axis. In another simulation study, we examined the cross-sectional changes in the distal carpal tunnel resulting from inward rotations of the hamate and trapezium [26]. Inward rotations of these bones around their centroids decreased the carpal arch width and increased the carpal arch area.

Effect of Repetitive Compression. Does the radio ulnar wrist compression improve functional outcome after repetitive compression? We investigated nerve conduction and patient reported

Fig. 7 Wearable brace with inflatable balloon bladder in the brace for radio ulnar wrist compression

outcomes after repetitive radio ulnar wrist compression using a pressure glove [27,28]. A portable, wearable wrist device was developed to reproduce the biomechanical specifications of our laboratory-based system [17,18]. The compression device consisted of a thermoformable Exos Wrist Brace with Boa (DJO, Vista, CA), capable of molding to the patient's wrist for a custom fit in an anatomically neutral position. An air bladder was attached to the inside of the brace. The bladder was centered around the hamate level on the ulnar side of the wrist. To inflate the bladder and apply wrist compression in the radio ulnar direction, an aneroid sphygmomanometer dial, bulb, and air valve was attached to the bladder via a rubber hose (Fig. 7).

Patients were trained to perform the wrist compression intervention protocol and instructions for use were provided for at-home reference for a 4-week intervention. During the four-week intervention period, patients performed three radio ulnar wrist compression sessions daily. Each session included three 5-min wrist compression intervals with a 1-min rest between intervals. A 10 N compressive force was achieved by inflating the bladder to a precalibrated pressure of 140 mmHg according to our previous study [18]. Patients were evaluated at Week 0 (baseline), Week 2 (midintervention) and Week 4 (end of intervention) for nerve conduction studies, cross-sectional area, mobility, and patient-reported outcomes. Patients showed decreased distal motor latency, cross-sectional area, and increased nerve mobility at Week 2 compared to baseline [28]. This study showed that the wrist compression intervention with 10 N force applied to the wrist in short term helped restore impaired morphological parameters and neurophysiological functions of the median nerve.

Patient reported outcomes included Boston Carpal Tunnel Questionnaire symptom and functional severity scales (BCTQ-SSS and BCTQ-FSS) [29] and symptoms of numbness/tingling based on Visual Analog Scales (VAS). We found that that wrist compression improved SSS by 0.55 points after two weeks and 0.51 points at four weeks compared to the baseline scale. At the four-week follow-up, SSS remained improved at 0.47 points [27]. Symptoms of numbness/tingling improved at two and four weeks, as well as the follow-up. Pain, numbness, and tingling had all improved by Week 2 of intervention. By Week 4, numbness and tingling remained improved relative to baseline, but improvements in pain at this time point did not reach significance (Table 1). We also obtained these patient-reported outcomes another 4 weeks (Week 8) after the intervention ended. At Week 8 follow up, numbness and tingling had improved relative to baseline, but pain scores had not changed. We also evaluated hand grip and pinch strengths, finding that motor function had a lower frequency across carpal tunnel syndrome sufferers and did not improve during the intervention or follow-up. Overall, we observed beneficial effects of the radio ulnar wrist compression intervention for the median nerve were evident after a relatively short period of 4 weeks of intervention, especially for alleviation of sensory related mechanisms and symptoms attributable to carpal tunnel syndrome. In particular, patients with mild to moderate severity in our study showed promising treatment effect to alleviate sensory symptoms. Future clinical trials are needed to optimize the force application dosage (duration, magnitude, and frequency) for carpal tunnel syndrome patients with various levels of symptom severity.

3 Muscle–Ligament Interaction for Carpal Arch Space Augmentation

Building upon the scientific and clinical premises of radio ulnar wrist compression (Fig. 8(b)), the second approach is to take advantage of the unique anatomical and biomechanical relationship between the thenar muscles and transverse carpal ligament. The origin of the thenar muscles on the volar side of the transverse carpal ligament [30,31] provides an opportunity to augment the

Table 1 Patient-reported outcome scores at weeks 0, 2, 4, and 8 (mean ± SD)

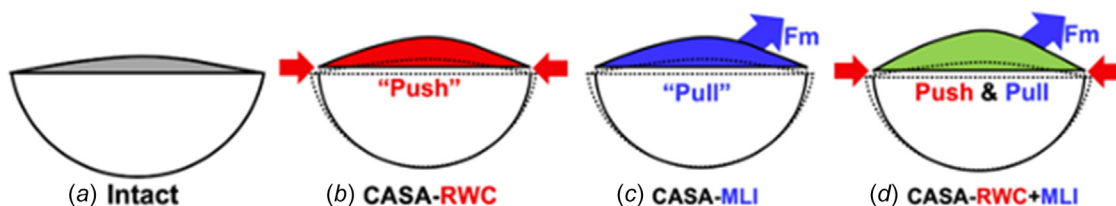|	Week 0	Week 2	Week 4	Week 8 Follow up
BCTQ-SSS	2.75 ± 0.67	2.20 ± 0.56	2.24 ± 0.50	2.28 ± 0.87
BCTS-FSS	2.11 ± 0.67	1.90 ± 0.51	1.83 ± 0.49	1.98 ± 0.81
VAS pain	5.31 ± 3.66	3.94 ± 2.72	4.06 ± 2.95	3.69 ± 3.48
VAS numbness	6.25 ± 2.70	4.06 ± 2.05	3.94 ± 2.17	3.69 ± 2.94
VAS tingling	5.44 ± 3.39	3.25 ± 2.21	3.38 ± 2.66	2.81 ± 2.56

Fig. 8 A geometrical illustration of the push (radio ulnar wrist compression (RWC)) and pull (muscle-ligament interaction (MLI)) mechanisms for CASA. F_m indicates thenar muscle force.
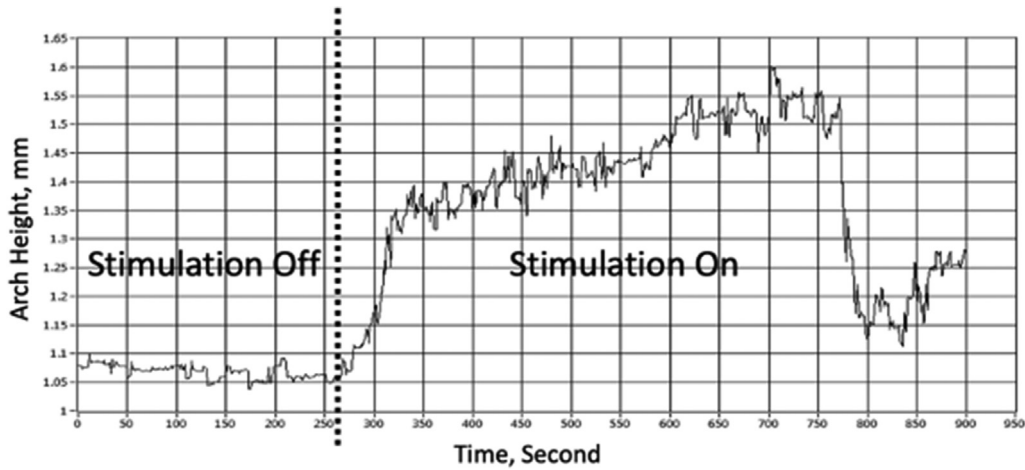
Fig. 9   Representative increase of carpal arch height without and with stimulation

ligament-formed carpal arch through muscle-ligament interaction (Fig. 8(*c*)). When the thenar muscles contract, forces are generated on the ligament in the volar direction, thus increasing the area under the transverse carpal ligament. The muscle-ligament interaction and radio ulnar wrist compression can act independently or synergistically to augment carpal arch space (Fig. 8(*d*)).

We investigated the biomechanical interaction between the transverse carpal ligament and the thenar muscles in live human subjects [32]. The morphological changes of the carpal arch in response to thenar muscle contractions were examined during isometric tip pinch between the thumb and index finger. Ultrasound videos of the carpal tunnel were recorded and synchronized with the forces measured by a pinch dynamometer. As the pinch force increased from 0 to 100% maximum voluntary contraction force, the carpal arch height increased and the carpal arch area increased. The transverse carpal ligament was pulled volarly during thenar muscle contractions, providing evidence for the biomechanical interaction between the ligament and muscles for CASA.

We use cadaveric hands to understand individual contributions of thenar muscles to carpal arch changes [33]. In this study, we pulled the adductor pollicis (APB), superficial head of flexor pollicis brevis (sFPB) and opponens pollicis (OPP) on the transverse carpal ligament formed carpal arch under force application by individual or combined muscles. Thenar muscles were loaded under 15% of their respective maximal force capacity, and ultrasound images of the cross section of the distal carpal tunnel were collected for morphometric analyses of the carpal arch. The arch height and area were dependent on the loading condition, muscle combination, and their interaction. The changes to arch height and area were dependent on the muscle combinations. The arch height and area increased under the loading combinations of APB, OPP, APB-sFPB, APB-OPP, or APB-sFPB-OPP, but not under the combinations of sFPB or sFPB-OPP. The carpal arch change under the APB-sFPB-OPP or APB-OPP loading was greater than that under the loading of APB-sFPB. This study demonstrated that thenar muscle forces exert biomechanical effects on the transverse carpal ligament to increase carpal arch height and area, and these increases were different for individual muscles and their combinations.

We have performed finite element analysis of the muscle-ligament interaction. We included only APB and OPP, as the FPB of the specimen was outside of the transverse carpal ligament. For this study, the stiffness structural properties were adopted from our previous studies [12,13]. We applied four force levels at 25%, 50%, 75%, and 100% of the maximum force capacities [34]. The force direction was determined as the vector from the centroid of the muscle attachment on the TCL to the muscle volume centroid. Both APB and OPP contractions increased arch area at the distal tunnel (APB, 9.7–13.2 mm^2; OPP, 13.1–16.0 mm^2). We also performed another finite element study showing carpal arch

enlargement with forces from radial to volar directions [35]. Volarly oriented forces were more favorable for greater carpal arch area which provided insights into the optimal positioning of the thumb to maximize space gain.

For a clinical application, we performed a preliminary study to examine carpal arch response to a range of stimulation intensities applied to the thenar muscles on hands [36]. We induced controlled isometric contractions of the thenar muscles using an electronic muscle stimulation device (InTENSity™, Austin, TX). Transcutaneous current was applied through electrodes with the cathode placed on the thenar muscle belly and the anode on the dorsum side of the lower arm proximal to the ulnar styloid process. For each of the subjects, we stimulated the thenar muscles at four different intensities (5, 6, 7, and 8 mA). Ultrasound videos of the carpal arch were collected at the distal tunnel level before and during stimulation. Carpal arch height increased, and the increases was greater as intensity increased. See an example of stimulation-response curve in Fig. 9. We also observed that the median nerve tended to become more rounded during stimulation.

4   Palmar Pulling by a Finite Element Model

A third approach to CASA is to apply external dorsal-to-volar force on the volar skin surface of the carpal tunnel region. The force influence may be propagated to the transverse carpal ligament through the connective tissues such as fat or muscles between the skin and ligament, bowing the ligament to enlarge the area under the carpal arch. We used a finite element model of the distal carpal arch (Fig. 10) to examine this force transmission and deformation effects [37,38].

A cadaveric hand was imaged by ultrasonography at the carpal tunnel to obtain a cross section at the hook of hamate level. The image was segmented to obtain the geometrical information of the
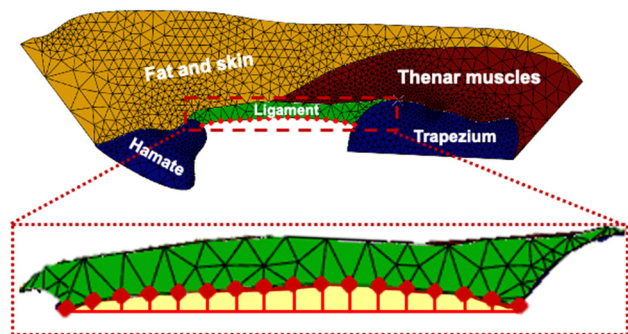

Fig. 10   Finite element model of the distal carpal arch

hamate, trapezium, thenar muscles, skin, fat, and transverse carpal ligament. Then the cross section was extruded with 1-mm thickness for a pseudo-three-dimensional object. The material properties of the muscle, fat and skin were adopted from the literature [39,40]. The ligament's anisotropic modulus was implemented by adding tension-only nonlinear springs to strengthen the transverse modulus. To compensate for the missing wrist bones, intercarpal ligaments and their functions, strings were added between the hamate and trapezium to simulate structural stiffness of the carpal arch based on a previous study [13]. As for boundary conditions, a tie constraint was set for all the interfaces with an assumption of no-slip contact. All components had displacement boundary condition free in-plane but fixed out-of-plane. We applied five levels of forces on the wrist (from 2 to 10 N), and analyzed the carpal arch area, height, and width.

The initial arch area without volarly applied forces was 13.15 mm^2. Arch area increased under volarly applied forces, and the area increased more as the force magnitude increased. The largest carpal arch area was 22.96 mm^2, at 10 N force application. Arch width, however, decreased under volarly applied forces. The largest decrease in arch width occurred at 10 N was 0.27 mm. The ligament was more bowed, shown by increases in the distance between nodes on the ligament volar surface and arch width line. All the nodes (except its two ends) on the ligament dorsal surface were volarly migrated, and the migration increased as the force magnitude increased. Displacement of the ligament was greatest at its midpoint and decreased toward the ligament's two ends. The finite element analysis demonstrated that the carpal arch can be expanded by volarly applying forces on the skin surface of the wrist. In the future, experimental studies are needed to refine and validate the computational model.

5 Collagenolysis of Transverse Carpal Ligament

The last approach is to explore a potential CASA method by injecting enzymes into the transverse carpal ligament to decrease the ligament stiffness to alleviate pressure off the median nerve. Collagenase injection has been an FDA approved procedure to regulate tissue stiffness in patients with Dupuytren's Contracture [41], a condition characterized by the thickening of the tissue causing irregular bending of the fingers. Similarly, reduction to the ligament's thickness and stiffness would facilitate its capability to elongate, expanding the carpal tunnel to decompress the median nerve.

Hypertrophy of the transverse carpal ligament has been anecdotally reported in patients with carpal tunnel syndrome [42–44]. It may be that repetitive hand use causes mechanical stimulation to the ligament by the thenar muscles and the flexor tendons, leading to the hypertrophy and fibrocartilaginous metaplasia of the ligament [45]. This postulation is supported by positive associations between carpal tunnel syndrome and high force-high repetition jobs [46]. Using acoustic radiation force impulse elastography, we examined in vivo mechanical properties of the transverse carpal ligament and found that the ligament had varying regional stiffnesses with greater values within the thenar muscle-attached region [47], and ligament increased stiffness in pianists [48] and carpal tunnel syndrome patients [49]. Ligament thickening may contribute to pathomechanics of the carpal tunnel which abnormally constrains the tunnel and compresses the median nerve.

We examined collagenase effect over time on the stiffness of the transverse carpal ligament specimens [50]. The ligament was dissected from cadaveric hands and 2 mm by 20 mm strips were placed into a petri dish containing 1500 Units of type I collagenase and 2 mL of solution. The control sample shows a steeper slope than the treatment ligament in general. The stiffness of the 1- and 2-h treatments are comparable, the stiffness of the ligament strip after 3-h treatment was reduced by 64% relative to the control. In another study, we determined the time- and dose-dependent effects of collagenase injection on elastic modulus and thickness in transverse carpal ligament specimens [51]. Transverse carpal ligament was dissected from cadaveric hands and
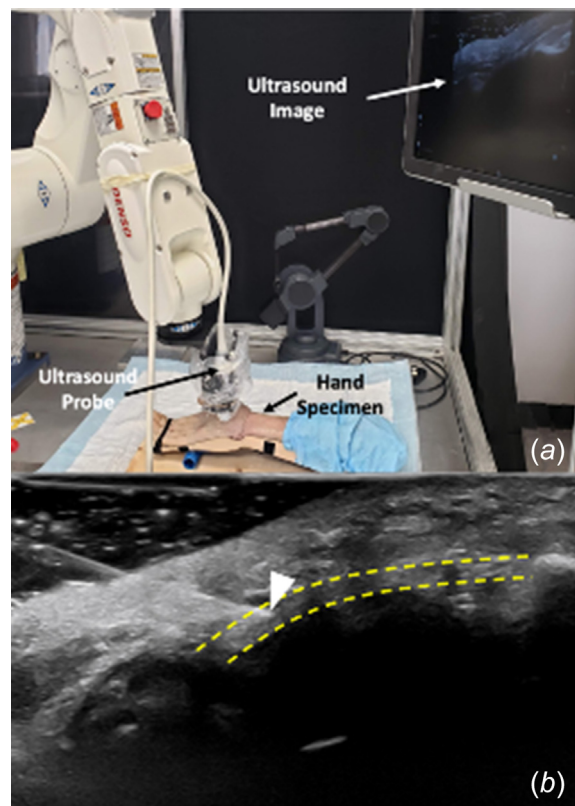

Fig. 11 Imaging the transverse carpal ligament for reconstruction (a) and robot-assisted insertion of the needle tip (indicated with white triangle) to the ligament (b)

doses of 50, 100, 150, 200, and 250 Units were injected into five points on the ligament, respectively. B-mode and shear wave elastography images were taken of each injection point using robot-assisted ultrasound imaging immediately after injection, as well as 2, 4, 6, 8, and 24 h after injection. Ligament thickness and mean shear wave speed were measured for each collagenase dose at each time point. Collagenase doses of 200 and 250 Units decreased shear wave speed by 18.70% and 30.01%, respectively, after 24 h. Collagenase doses of 150, 200, and 250 Units decreased ligament thickness by 7.28%, 10.97%, and 14.92%, respectively, after 24 h. Our findings suggest that collagenase injection may be used to degrade the transverse carpal ligament, with higher doses of collagenase resulting in greater tissue degradation up to 24 h after injection.

Due to the small size of the transverse carpal ligament, which has a thickness within 3.0 mm [52], accuracy of needle placement is needed to ensure proper delivery of collagenase and prevent damage to surrounding structures. We determined specimen-specific anatomic reconstruction of the ligament, and then inserted the needle to the middle of the ligament thickness [53]. Robot-assisted ultrasonography [54] was used for the reconstruction (Fig. 11(a)). Each injection was delivered by rigidly fixing a 27-gauge needle to a robot arm programed to insert the needle tip to the intended target. Ultrasound images were taken of the needle inserted into the ligament to measure accuracy and precision of the needle placement. The needle tip was successfully delivered to the middle region of the ligament thickness and visualized using ultrasound imaging (Fig. 11(b)). The accuracy and precision of the needle insertion were 0.83 and 0.31 mm, respectively. This established the subject-specific methodology to be used in the future to deliver enzymatic injections to the ligament.

6 Summary

Carpal tunnel syndrome is extremely common, and transecting the transverse carpal ligament is the standard surgical treatment.

This paper reviewed our approaches to the treatment of carpal tunnel syndrome by nonsurgical approaches. The carpal tunnel geometrical models characterized the transverse carpal ligament using triangle, parabolic, and constant perimeter, and all models showed that there was an increase in cross-sectional area with arch width narrowing or shape change. Experimental approaches demonstrated that the carpal tunnel was biomechanically manipulatable for carpal arch space augmentation to reduce the compression on the median nerve and relieve symptoms of carpal tunnel syndrome. These approaches have sound scientific rationale with arch width narrowing or shape change demonstrating promising patient reported outcomes for clinical translation, while collagenolysis of the transverse carpal ligament are exploratory. It is our hope that, through rigorous theoretical and applied research, evidence-based nonsurgical solutions will become available for countless sufferers with carpal tunnel syndrome.

References

[1] Prantil, R. K., Xiu, K., Kim, K. E., Gaitan, D. M., Sacks, M. S., Woo, S. L., and Li, Z. M., 2012, "Fiber Orientation of the Transverse Carpal Ligament," Clin Anat., **25**(4), pp. 478–482.

[2] Papanicolaou, G. D., McCabe, S. J., and Firrell, J., 2001, "The Prevalence and Characteristics of Nerve Compression Symptoms in the General Population," J. Hand Surg., **26**(3), pp. 460–466.

[3] Atroshi, I., Gummesson, C., Johnsson, R., Ornstein, E., Ranstam, J., and Rosen, I., 1999, "Prevalence of Carpal Tunnel Syndrome in a General Population," JAMA, **282**(2), pp. 153–158.

[4] Huisstede, B. M., Hoogvliet, P., Randsdorp, M. S., Glerum, S., van Middelkoop, M., and Koes, B. W., 2010, "Carpal Tunnel Syndrome. Part I: Effectiveness of Nonsurgical Treatments–a Systematic Review," Arch. Phys. Med. Rehabil., **91**(7), pp. 981–1004.

[5] Kato, T., Kuroshima, N., Okutsu, I., and Ninomiya, S., 1994, "Effects of Endoscopic Release of the Transverse Carpal Ligament on Carpal Canal Volume," J. Hand Surg., **19**(2), pp. 416–419.

[6] Fuss, F. K., and Wagner, T. F., 1996, "Biomechanical Alterations in the Carpal Arch and Hand Muscles After Carpal Tunnel Release: A Further Approach Toward Understanding the Function of the Flexor Retinaculum and the Cause of Postoperative Grip Weakness," Clin. Anat., **9**(2), pp. 100–108.

[7] Guo, X., Fan, Y., and Li, Z. M., 2009, "Effects of Dividing the Transverse Carpal Ligament on the Mechanical Behavior of the Carpal Bones Under Axial Compressive Load: A Finite Element Study," Med. Eng. Phys., **31**(2), pp. 188–194.

[8] Brooks, J. J., Schiller, J. R., Allen, S. D., and Akelman, E., 2003, "Biomechanical and Anatomical Consequences of Carpal Tunnel Release," Clin. Biomech. (Bristol, Avon), **18**(8), pp. 685–693.

[9] Kiritsis, P. G., and Kline, S. C., 1995, "Biomechanical Changes After Carpal Tunnel Release: A Cadaveric Model for Comparing Open, Endoscopic, and Step-Cut Lengthening Techniques," J. Hand Surg., **20**(2), pp. 173–180.

[10] Li, Z. M., Tang, J., Chakan, M., and Kaz, R., 2009, "Carpal Tunnel Expansion by Palmarly Directed Forces to the Transverse Carpal Ligament," ASME J. Biomech. Eng., **131**(8), p. 081011.

[11] Gabra, J. N., Kim, D. H., and Li, Z. M., 2015, "Elliptical Morphology of the Carpal Tunnel Cross Section," Eur. J. Anat., **19**(1), pp. 49–56.

[12] Xiu, K. H., Kim, J. H., and Li, Z. M., 2010, "Biomechanics of the Transverse Carpal Arch Under Carpal Bone Loading," Clin. Biomech. (Bristol, Avon), **25**(8), pp. 776–780.

[13] Gabra, J. N., and Li, Z. M., 2016, "Three-Dimensional Stiffness of the Carpal Arch," J. Biomech., **16**(2), pp. 53–59.

[14] Gabra, J. N., Domalain, M., and Li, Z. M., 2012, "Movement of the Distal Carpal Row During Narrowing and Widening of the Carpal Arch Width," ASME J. Biomech. Eng., **134**(10), p. 101004.

[15] Li, Z. M., Gabra, J. N., Marquardt, T. L., and Kim, D. H., 2013, "Narrowing Carpal Arch Width to Increase Cross-Sectional Area of Carpal Tunnel–A Cadaveric Study," Clin. Biomech. (Bristol, Avon), **28**(4), pp. 402–407.

[16] Kim, D. H., Marquardt, T. L., Gabra, J. N., Shen, Z. L., Evans, P. J., Seitz, W. H., and Li, Z. M., 2013, "Pressure-Morphology Relationship of a Released Carpal Tunnel," J. Orthop. Res., **31**(4), pp. 616–620.

[17] Marquardt, T. L., Gabra, J. N., and Li, Z. M., 2015, "Morphological and Positional Changes of the Carpal Arch and Median Nerve During Wrist Compression," Clin. Biomech. (Bristol, Avon), **30**(3), pp. 248–253.

[18] Marquardt, T. L., Evans, P. J., Seitz, W. H., Jr., and Li, Z. M., 2016, "Carpal Arch and Median Nerve Changes During Radioulnar Wrist Compression in Carpal Tunnel Syndrome Patients," J. Orthop. Res., **34**(7), pp. 1234–1240.

[19] Luchetti, R., Schoenhuber, R., De Cicco, G., Alfarano, M., Deluca, S., and Landi, A., 1989, "Carpal-Tunnel Pressure," Acta Orthop. Scand., **60**(4), pp. 397–399.

[20] Gelberman, R. H., Aronson, D., and Weisman, M. H., 1980, "Carpal-Tunnel Syndrome. Results of a Prospective Trial of Steroid Injection and Splinting," J. Bone Jt. Surg. Am., **62**(7), pp. 1181–1184.

[21] Okutsu, I., Ninomiya, S., Hamanaka, I., Kuroshima, N., and Inanami, H., 1989, "Measurement of Pressure in the Carpal Canal Before and After Endoscopic Management of Carpal Tunnel Syndrome," J. Bone Jt. Surg. Am., **71**(5), pp. 679–683.

[22] Li, Z. M., Marquardt, T. L., Gabra, J. N., Evans, P. J., Seitz, W. H., and Diao, E., 2016, "In Vivo Reduction in Carpal Tunnel Pressure During Radioulnar Wrist Compression," Annual Meeting of the Orthopaedic Research Society, Orlando, FL, Mar. 5–8.

[23] Yao, Y., Grandy, E. L., Evans, P. J., Seitz, W. H., and Li, Z. M., 2018, "Enhancement in Median Nerve Mobility During Radioulnar Wrist Compression in Carpal Tunnel Syndrome Patients," Clin. Biomech. (Bristol, Avon), **60**, pp. 83–88.

[24] Yao, Y., Grandy, E., Evans, P. J., Seitz, W. H., Jr., and Li, Z. M., 2020, "Location-Dependent Change of Median Nerve Mobility in the Carpal Tunnel of Patients With Carpal Tunnel Syndrome," Muscle Nerve, **62**(4), pp. 522–527.

[25] Walia, P., Erdemir, A., and Li, Z. M., 2017, "Subject-Specific Finite Element Analysis of the Carpal Tunnel Cross-Sectional to Examine Tunnel Area Changes in Response to Carpal Arch Loading," Clin. Biomech. (Bristol, Avon), **42**, pp. 25–30.

[26] Jordan, D., and Li, Z. M., 2022, "Cross-Sectional Changes of the Distal Carpal Tunnel With Simulated Carpal Bone Rotation," Comput. Methods Biomech. Biomed. Eng., **25**(14), pp. 1599–1607.

[27] Li, Z. M., Grandy, E. L., Jenkins, L., Norman, C., Bena, J., Hou, J., Evans, P. J., Seitz, W. H., and Kwoh, C. K., 2022, "A Preliminary Study of Clinical Effectiveness of Radioulnar Wrist Compression in Treating Carpal Tunnel Syndrome," BMC Musculoskeletal Disord., **23**, p. 971.

[28] Yao, Y., Grandy, E., Jenkins, L., Hou, J., Evans, P. J., Seitz, W. H., Jr., and Li, Z. M., 2019, "Changes of Median Nerve Conduction, Cross-Sectional Area and Mobility by Radioulnar Wrist Compression Intervention in Patients With Carpal Tunnel Syndrome," J. Orthop. Transl., **18**, pp. 13–19.

[29] Levine, D. W., Simmons, B. P., Koris, M. J., Daltroy, L. H., Hohl, G. G., Fossel, A. H., and Katz, J. N., 1993, "A Self-Administered Questionnaire for the Assessment of Severity of Symptoms and Functional Status in Carpal Tunnel Syndrome," J. Bone Jt. Surg. Am., **75**(11), pp. 1585–1592.

[30] Loss, J., and Li, Z. M., 2020, "Biometry of Thenar Muscle Origins on the Flexor Retinaculum," Clin. Anat., **33**(8), pp. 1176–1180.

[31] Alsafar, F., and Li, Z. M., 2022, "Thenar and Hypothenar Muscle Coverage on the Transverse Carpal Ligament," J. Wrist Surg., **11**(2), pp. 150–153.

[32] Shen, Z. L., and Li, Z. M., 2013, "Biomechanical Interaction Between the Transverse Carpal Ligament and the Thenar Muscles," J. Appl. Physiol., **114**, pp. 225–229.

[33] Zhang, H., Loss, J., and Li, Z. M., 2021, "Carpal Arch Changes in Response to Thenar Muscle Loading," ASME J. Biomech. Eng., **143**(10), p. 101003.

[34] Zhang, H., Yao, Y., and Li, Z. M., 2019, "Three-Dimensional Finite Element Analysis of Transverse Carpal Ligament Under Simulated Thenar Muscle Contraction," The Annual Meeting of the Orthopaedic Research Society, Austin, TX, Feb. 2–5.

[35] Zhang, H., and Li, Z. M., 2021, "Finite Element Analysis for Carpal Arch Under Varying Thenar Muscle Force Magnitudes and Directions," Summer Biomechanics, Bioengineering and Biotransport Conference (SB3C), Virtual, June 14–18.

[36] Zhang, H., Rudy, M., and Li, Z. M., 2020, "Carpal Arch Changes by Transcutaneous Electrical Stimulation of the Thenar Muscles," International Symposium on Ligaments & Tendons (ISL&T – XVIII), Phoenix, AZ, Feb. 7.

[37] Zhang, H., and Li, Z. M., 2022, "Carpal Arch Space Augmentation by Volarly Applied Force on the Skin Surface – A Finite Element Study," Summer Biomechanics, Bioengineering and Biotransport Conference (SB3C), Chesapeake Bay Resort, MD, June 20–23.

[38] Yao, Y., Erdemir, A., and Li, Z. M., 2018, "Finite Element Analysis for Transverse Carpal Ligament Tensile Strain and Carpal Arch Area," J. Biomech., **73**, pp. 210–216.

[39] Palevski, A., Glaich, I., Portnoy, S., Linder-Ganz, E., and Gefen, A., 2006, "Stress Relaxation of Porcine Gluteus Muscle Subjected to Sudden Transverse Deformation as Related to Pressure Sore Modeling," ASME J. Biomech. Eng., **128**(5), pp. 782–787.

[40] Brosh, T., and Arcan, M., 2000, "Modeling the Body/Chair Interaction - An Integrative Experimental-Numerical Approach," Clin. Biomech. (Bristol, Avon), **15**(3), pp. 217–219.

[41] Hurst, L. C., Badalamente, M. A., Hentz, V. R., Hotchkiss, R. N., Kaplan, F. T., Meals, R. A., Smith, T. M., Rodzvilla, J., and Group, C. I. S., 2009, "Injectable Collagenase clostridium histolyticum for Dupuytren's Contracture," N. Engl. J. Med., **361**(10), pp. 968–979.

[42] John, V., Nau, H. E., Nahser, H. C., Reinhardt, V., and Venjakob, K., 1983, "CT of Carpal Tunnel Syndrome," AJNR Am. J. Neuroradiol., **4**(3), pp. 770–772.

[43] Yamagami, T., Higashi, K., Handa, H., Minouchi, K., Fujii, M., Nishihara, K., and Kaji, R., 1994, "Carpal Tunnel Syndrome: Clinical Experience of 61 Cases," No Shinkei Geka, **22**(7), pp. 617–620.

[44] Ferrari, F. S., Della Sala, L., Cozza, S., Guazzi, G., Belcapo, L., Mariottini, A., Bolognini, A., and Stefani, P., 1997, "High-Resolution Ultrasonography in the Study of Carpal Tunnel Syndrome," Radiol. Med. (Torino), **93**(4), pp. 336–341.

[45] Moore, J. S., 2002, "Biomechanical Models for the Pathogenesis of Specific Distal Upper Extremity Disorders," Am. J. Ind. Med., **41**(5), pp. 353–369.

[46] Silverstein, B. A., Fine, L. J., and Armstrong, T. J., 1987, "Occupational Factors and Carpal Tunnel Syndrome," Am. J. Ind. Med., **11**(3), pp. 343–358.

[47] Shen, Z. L., Vince, D. G., and Li, Z. M., 2013, "In Vivo Study of Transverse Carpal Ligament Stiffness Using Acoustic Radiation Force Impulse (ARFI) Imaging," PLoS One, **8**(7), p. e68569.

[48] Mhanna, C., Marquardt, T. L., and Li, Z. M., 2016, "Adaptation of the Transverse Carpal Ligament Associated With Repetitive Hand Use in Pianists," PLoS One, **11**(3), p. e0150174.

[49] Marquardt, T. L., Gabra, J. N., Evans, P. J., Seitz, W. H., and Li, Z. M., 2016, "Thickness and Stiffness Adaptations of the Transverse Carpal Ligament Associated With Carpal Tunnel Syndrome," J. Musculoskeletal Res., **19**(4), p. 1650019.

[50] Prantil, R. K., Mondello, T. A., Yu, S. H., Pervaiz, K., Woo, S. L.-Y., and Li, Z. M., 2013, "Stiffness of the Transverse Carpal Ligament Under the Influence of Collagenase," ASME Paper No. SBC2011-53284.

[51] Hawk, J., Daulat, S., Margolis, D., and Li, Z. M., 2022, "Dose- and Time-Dependent Effects of Collagenase Clostridium Histolyticum Injection on Stiffness and Thickness of In Vitro Transverse Carpal Ligament," Summer Biomechanics, Bioengineering and Biotransport Conference (SB3C), Chesapeake Bay Resort, MD, June 20–23.

[52] Pacek, C. A., Chakan, M., Goitz, R. J., Kaufmann, R. A., and Li, Z. M., 2010, "Morphological Analysis of the Transverse Carpal Ligament," Hand (NY), **5**(2), pp. 135–140.

[53] Hawk, J., Daulat, S., Margolis, D., and Li, Z. M., 2022, "Ultrasonographic 3D Reconstruction of and Robot-Assisted Injection to the Transverse Carpal Ligament," North American Congress on Biomechanics (NACOB), Ottawa, ON, Canada, Aug. 21–25.

[54] Shah, R., and Li, Z. M., 2022, "Three-Dimensional Carpal Arch Morphology Using Robot-Assisted Ultrasonography," IEEE Trans. Biomed. Eng., **69**(2), pp. 894–898.